Development 126, 1891-1902 (1999)
Printed in Great Britain © The Company of Biologists Limited 1999
DEV8570

Sensory activity affects sensory axon development in *C. elegans*

Erin L. Peckol, Jennifer A. Zallen, Justin C. Yarrow and Cornelia I. Bargmann*

Howard Hughes Medical Institute, Department of Anatomy and Department of Biochemistry and Biophysics, University of California, San Francisco, CA 94143-0452, USA
*Author for correspondence (e-mail: cori@itsa.ucsf.edu)

Accepted 9 February; published on WWW 6 April 1999

SUMMARY

The simple nervous system of the nematode *C. elegans* consists of 302 neurons with highly reproducible morphologies, suggesting a hard-wired program of axon guidance. Surprisingly, we show here that sensory activity shapes sensory axon morphology in *C. elegans*. A class of mutants with deformed sensory cilia at their dendrite endings have extra axon branches, suggesting that sensory deprivation disrupts axon outgrowth. Mutations that alter calcium channels or membrane potential cause similar defects. Cell-specific perturbations of sensory activity can cause cell-autonomous changes in axon morphology. Although the sensory axons initially reach their targets in the embryo, the mutations that alter sensory activity cause extra axon growth late in development. Thus, perturbations of activity affect the maintenance of sensory axon morphology after an initial pattern of innervation is established. This system provides a genetically tractable model for identifying molecular mechanisms linking neuronal activity to nervous system structure.

Key words: *C. elegans*, Sensory neurons, Activity-dependent development, axon outgrowth

INTRODUCTION

Activity-dependent processes provide a method by which neuronal connections can be refined purely based on the information that they convey (Shatz, 1994, 1996). These mechanisms were first discovered through their roles in plasticity of the postnatal vertebrate nervous system, and have subsequently proved to have widespread functions in neuronal development (Hubel et al., 1977; Shatz and Stryker, 1978; Goodman and Shatz, 1993). The effects of activity are best characterized in vertebrate sensory systems, where large groups of axons use activity patterns to refine connections to their target regions.

The nervous system of the nematode *C. elegans* is simple and highly stereotyped; each of its 302 neurons has a predictable axon morphology and characteristic synaptic connections (White et al., 1986). Although some variation in synapses was observed between animals, the near-invariance of this pattern suggests the existence of a reproducible developmental program that defines neuronal connectivity. Nonetheless, the possibility of activity-dependent processes in *C. elegans* sensory development was raised by the properties of the sensory mutants *tax-2* and *tax-4*. The *tax-2* and *tax-4* genes are required for normal olfaction, taste and thermosensation, and they encode a cyclic nucleotide-gated channel with extensive similarity to the vertebrate visual and olfactory sensory transduction channels (Coburn and Bargmann, 1996; Komatsu et al., 1996). Interestingly, animals with *tax-2* or *tax-4* mutations exhibit axon defects in chemosensory neurons; some neurons have extra axon branches or axons that fail to terminate at their normal positions (Coburn and Bargmann, 1996). Two general models could explain these results. The cyclic nucleotide-gated channel could participate directly in an axon outgrowth pathway in sensory neurons. Alternatively, the axon defects in *tax-2* and *tax-4* mutants could be an indirect consequence of altered sensory activity in the absence of the sensory transduction channel.

Several properties of the *tax-2* and *tax-4* mutants indicate that the cyclic nucleotide-gated channel acts in the maintenance of axon morphology, and not in initial axon guidance events. The sensory axons first extend to their targets in the embryo (Sulston et al., 1983), but the aberrant axon branches in *tax-2* and *tax-4* mutants do not appear until later larval stages, suggesting a late time of action (Coburn et al., 1998). Indeed, conditional mutations in *tax-2* reveal that this gene is required even in the adult stage to maintain correct axon morphologies (Coburn et al., 1998). By contrast, more conventional sensory axon guidance molecules are only required during embryogenesis, consistent with a function in sensory pathfinding (Zallen et al., 1998). The late requirement for *tax-2* and *tax-4* is reminiscent of the later effects of activity in vertebrate sensory development.

Here we use a set of genetic manipulations to ask whether activity affects the outgrowth of sensory axons in *C. elegans*, a question that has not been addressed directly in the past. We examine the development of chemosensory neurons in the two amphid sensory organs that respond to chemical, thermal and mechanical stimulation (Ward et al., 1975; Ware et al., 1975; Bargmann and Mori, 1997). We demonstrate that normal sensory inputs are required for normal axon morphology in a subset of sensory neurons, and that voltage-activated channels

participate in maintaining axon morphology. Silencing a single neuron can lead to cell-autonomous effects on its axon growth. As in *tax-2* and *tax-4* mutants, these effects are observed only late in development, not in initial axon pathfinding. These results demonstrate that axon morphology in *C. elegans* is sensitive to changes in activity, revealing a conserved and perhaps ancient role of activity in plasticity and growth of sensory systems.

MATERIALS AND METHODS

Strains and genetics

Wild-type nematodes were *C. elegans* variety Bristol, strain N2, grown under standard uncrowded and well-fed conditions at 25°C unless otherwise noted (Brenner, 1974). Table 1 provides strain information for this work. The integrated *tax-2p::GFP* fusion gene used to visualize the ASE neurons is expressed in AFD, ASE, ASI, AWC, BAG and AQR (Coburn and Bargmann, 1996; Coburn et al., 1998). The integrated *tax-2Δ::GFP* fusion gene used to visualize the ASJ neurons is expressed in ASG, ASI, ASJ, ASK, AWB and AWC. Several other GFP fusion genes that label either pairs of cells or single cells were used to examine individual cell morphology in detail. These included two integrated fusion genes, *str-1::GFP* (AWB) and *str-3::GFP* (ASI), and two fusion genes maintained as unstable arrays, *gcy-5::GFP* (right ASE) and *gcy-7::GFP* (left ASE) (generously provided by David Garbers and Leon Avery) (Troemel et al., 1995, 1997; Yu et al., 1997).

Animals were scored for the morphology of a given neuron type and those with at least one ectopic axon in a neuron pair were scored as defective. Statistical analysis was conducted using Primer of Biostatistics software (Stanton A. Glantz, McGraw Hill publishers). Confocal images were acquired using LaserSharp Acquisition Version 2.1A software (BioRad), an Optiphot-2 microscope (Nikon), and the Laser Scanning Confocal Imaging System MRC-1024 (BioRad). Epifluorescence images were acquired using an Axioplan 2 (Zeiss).

Behavioral assays

Population chemotaxis assays were performed as described (Bargmann et al., 1993). The dilution of the odorant benzaldehyde in ethanol was 1:200. The chemotaxis index (n) was defined as $(n_{attractant} - n_{counterattractant})/n_{total}$. Statistical significance was determined using Student's *t*-test. Osmotic avoidance assays and nose touch assays were performed as described (Vowels and Thomas, 1994; Kaplan and Horvitz, 1993).

Molecular biology

Transcriptional fusions between the *sra-6* promoter and Kv1.1 and Kv1.2 were constructed using expression vectors generously provided by Andrew Fire. A 4 kb *sra-6* promoter was amplified by PCR from *C. elegans* genomic DNA (Expand PCR kit, Boehringer Mannheim), using primers that created *Bam*HI sites, and was cloned into the *Bam*HI site of the GFP expression vector pPD95.75, yielding the *sra-6::GFP* transcriptional fusion gene. *sra-6::Kv1.1* and *sra-6::Kv1.2* were constructed from *sra-6::GFP* by replacing the GFP coding sequence with cDNAs for RCK1 (Kv1.1) or RCK5 (Kv1.2) (Baumann et al., 1988; Tempel et al., 1988; Stuhmer et al., 1989; constructs generously provided by D. McKinnon). *sra-6::Kv1.1* (10 μg/ml) and *sra-6::Kv1.2* (50 μg/ml) were coinjected with plasmid pJM23(*lin-15*) (50 μg/ml) into the gonads of *lin-15(n765ts)* animals (Herman and Hedgecock, 1990; Huang et al., 1994). The *sra-6::Kv1.1* construct was injected at a lower concentration because Kv1.1 is activated at less depolarized potentials than Kv1.2 (Grissmer et al., 1994). Transgenic animals were identified by the rescue of the *lin-15(n765ts)* multivulval phenotype at 20°C. Transgenes were integrated into *lin-15(n765ts)* by trimethylpsoralen and ultraviolet irradiation (A. Santoso, N. L'Etoile and C. I. B., unpublished results) to generate the *sra-6::Kv1.1* and *sra-6::Kv1.2* integrated strains. Independent

Table 1. GFP fusion genes used to visualise sensory neurons

		ASER/ASEL	ASE pair	ASI pair	ASJ pair	AWB pair
		gcy-5::GFP ASER DA1262 *gcy-7::GFP* ASEL DA1288	*tax-2p::GFP* IV CX3589	*str-3::GFP* X CX3596	*tax-2Δ::GFP* IV CX3797	*str-1::GFP* X CX3553
che-3(e1124) I	CB1124	CX3986 ASER	CX3825	CX3608	CX3826	CX3979
che-11(e1810) V	CB3330	CX3959 ASER	CX3817	CX3612	CX3829	CX3978
daf-6(e1377) X	CB1377	CX3965 ASEL CX3962 ASER	CX4167	CX3967	CX3919	CX3977
eat-6(ad497) V	DA467	CX3961 ASER	n.d.	CX3599	CX3918	CX4169
egl-19(ad695) IV	DA695	CX3927 ASER	CX3921	CX3601	CX3922	CX3890
osm-1(p808) X	PR808	CX3928 ASER	CX4166	CX4173	CX3920	CX3974
osm-5(p813) X	PR813	CX3966 ASEL	CX3828	CX4172	CX3827	CX4168
osm-6(p811) V	PR811	n.d.	CX3985	CX3605	CX3830	CX3983
snt-1(md290) II	RM1613	n.d.	CX3816	CX3801	CX3799	n.d.
tax-2(p691) I	CX2217	n.d.	CX3814	CX4171	CX3988	CX3973
tax-4(p678) III	CX2948	CX3963 ASER	CX4165	CX4170	CX3987	CX3982
unc-13(e51) I	CX2039	n.d.	CX3804	CX3800	CX3806	CX3984
unc-18(e81) dpy-6(e14) X		n.d.	CX3813	CX3815	CX3808	n.d.
unc-36(e251) III	CB251	CX3960 ASER	CX3597	CX3802	CX3809	CX3972
unc-104(e1265) II	CB1265	n.d.	CX3811	CX3807	CX3798	n.d.

A set of GFP fusion genes was used to visualize sensory neurons. See text for details.

n.d., not done.

Additional classes of axons were examined using other GFP fusion genes: *daf-6(e1377), che-14(e1960), osm-1(p808), che-11(e1810), osm-6(p811),* and *daf-19(m86)* were examined using *ceh-23::GFP* (for the ADF, ADL, AFD, ASE, ASG, ASH, ASI, and AWC neuron pairs); *osm-6(p811)* and *osm-5(p813)* were examined using *sra-6::GFP* (for the ASH neuron pair); *osm-6(p811)* and *che-3(e1124)* were examined using *odr-10::GFP* (for the AWA neuron pair); and *osm-6(p811), che-3(e1124), eat-6(ad497),* and *egl-19(ad695)* were examined using *str-2::GFP* (for the AWC neurons) (Troemel et al., 1995; Sengupta et al., 1996; Troemel et al., 1997 and E.R. and C.I.B., unpublished results) . No extra axons were observed extending from these neurons, except with the *ceh-23::GFP* fusion gene where the ectopic axons could be accounted for by ASE and ASI defects. Finally, integrated strains carrying either the *sra-6::Kv1.1* (CX3821, CX3822) or *sra-6::Kv1.2* (CX3818, CX3819, CX3820) transgene were examined for extra axons using *sra-6::GFP* (ASH), *str-3::GFP* (ASI), and *tax-2Δ::GFP* (ASJ).

integration events yielded 2 *sra-6::Kv1.1* lines and 3 *sra-6::Kv1.2* lines. All lines yielded similar results.

A version of the *sra-6::Kv1.2* plasmid that encodes a non-conducting channel was constructed by replacing GYG of the pore-forming loop (H5) with AAA (Tinker et al., 1996), yielding *sra-6::Kv1.2AAA*. Site-directed mutagenesis was performed using the Stratagene QuikChange Kit and mutations were confirmed by sequencing.

Transcriptional fusions between the *glr-1* promoter and Kv1.1 and Kv1.2 were constructed by cloning a *Pst*I/*Bam*HI fragment containing the *glr-1* promoter from a *glr-1::gfp* gene (Maricq et al., 1995) into the expression vector pPD49.26. The Kv1.1 and Kv1.2 cDNAs were then subcloned into a *Sac*I site. *glr-1::Kv1.1* (50 μg/ml) and *glr-1::Kv1.2* (50 μg/ml) were each coinjected with the plasmid pJM23(*lin-15*) (50 μg/ml) into the gonads of *glr-1::gfp; lin-15(n765ts)* animals.

To express the *eat-6* cDNA specifically in ASER, a transcriptional fusion between the *gcy-5* promoter and the *eat-6* cDNA (yk470c9, generously provided by Yuji Kohara) was constructed using the expression vector pPD49.26. 2.7 kb of *gcy-5* promoter sequence was amplified from genomic DNA using primers that created *Sph*I and *Bam*HI sites, and subcloned into pPD49.26. *gcy-5::eat-6* was constructed by subcloning the *Pvu*I/*Pst*I fragment of the *eat-6* cDNA (blunt-ended with T4 DNA polymerase) into the *Sma*I site in pPD49.26. The *eat-6* coding region was sequenced to confirm absence of mutations. *gcy-5::gfp* (50 μg/ml) and the plasmid pJM23(*lin-15*) (50 μg/ml) were injected either with or without *gcy-5::eat-6* (50 μg/ml) into the gonads of *lin-15(n765ts)* and *eat-6(ad497); lin-15(n765ts)* animals.

Antibody staining of Kv1.1 and Kv1.2 proteins

Integrated lines expressing the *sra-6::Kv1.1* and *sra-6::Kv1.2* fusion genes were stained with antibodies against the channel proteins (Alomone Labs). Adult hermaphrodites were washed with M9 saline and dropped onto 0.1% polylysine-coated slides. The animals were heat-fixed at 100°C for 20 seconds, processed for antibody staining using freeze-fracture and methanol-acetone fixation, and stained using standard techniques (Miller and Shakes, 1995). Primary antibodies were used at a dilution of 1:100, and an FITC-conjugated goat α-rabbit secondary antibody was used at 1:50 (Jackson ImmunoResearch Labs, Inc.).

RESULTS

tax-2 and *tax-4* mutants have extra sensory axon branches

C. elegans amphid sensory neurons have a bipolar morphology with one axon and one dendrite each (Ward et al., 1975; Ware et al., 1975; White et al., 1986; Fig. 1). The dendrite connects to an anterior opening, where it terminates in a sensory cilium, and the axon extends into a bundle called the nerve ring, where it makes synapses onto other neurons. Each of the two bilaterally symmetric amphid organs contains 12 neurons whose axons always project in the region anterior to their cell bodies. In *tax-2* and *tax-4* cyclic nucleotide-gated channel mutants, vital staining with the fluorescent dye DiO revealed extra ventral posterior axon branches extending from the two ASJ sensory neurons (Coburn and Bargmann, 1996; Coburn et al., 1998). GFP fusion genes that labeled subsets of amphid sensory neurons revealed defects in some additional neurons, including the ASE, AWB and ASI neurons (Fig. 1 and data not shown).

Are the misplaced axons caused by guidance defects or by excess axon growth? To characterize the *tax-2* and *tax-4* axon phenotypes more carefully, we examined the axons of several sensory neurons using GFP fusion genes that are expressed in only a single neuron or in only one pair of neurons. This analysis revealed that the ASE, ASI and AWB neurons in *tax-2* and *tax-4* mutants all had ectopic lateral posterior axons that extended directly from the cell body in addition to an apparently normal axon that extended into the nerve ring (Figs 1, 2, and data not shown). Since *tax-2* and *tax-4* mutants have ectopic axons or axon branches together with superficially normal nerve ring axons, their primary defect appears to be inappropriate axon initiation, growth or branching rather than initial axon guidance.

tax-2 and *tax-4* mutants have profound defects in AWB, ASE and ASI sensory function (Coburn and Bargmann, 1996; Troemel et al., 1997; our data not shown), but the AWB and ASI axon defects were present at a low frequency even in *tax-4* null mutants (Fig. 2). Thus the observed axon defects are mild compared to the behavioral defects in the mutants. These results are consistent either with a direct role for *tax-2* and *tax-4* in axon outgrowth, or with an indirect role in outgrowth via TAX-2/TAX-4 effects on sensory transduction. Standard genetic or molecular methods cannot easily distinguish between these possibilities, especially since TAX-2::GFP protein can be observed in sensory cilia, axons and cell bodies (Coburn and Bargmann, 1996). However, the model that sensory transduction affects axon outgrowth can be tested independently, and we have taken this approach below.

Mutants with defective sensory cilia have ectopic sensory axons

In vertebrate sensory systems, effects of activity can be revealed by sensory deprivation: segregation of ocular dominance columns is disrupted by closing the eyes and, in rodents, whisker barrel cortex is disrupted by trimming the sensory whiskers (LeVay et al., 1980; Harris and Woolsey, 1981; Crair et al., 1998). *C. elegans* is too small for analogous surgical manipulations, but a physical obstruction of the chemosensory organs can be produced by certain mutations. Mutations in at least 25 cilium structure genes cause morphological defects in the sensory cilia or the support cells (the socket and sheath) that form the sensory pore (Perkins et al., 1986; Starich et al., 1995). The stunted or occluded cilia lack access to extracellular chemical stimuli, providing essentially the equivalent of a block of the pore. Six different cilium structure mutants were examined to investigate whether sensory deprivation leads to defective sensory axon structure: *daf-6*, which acts within the amphid support sheath that surrounds the cilia, *osm-6*, which encodes a protein that is strictly localized to cilia, and *che-3*, *che-11*, *osm-1* and *osm-5* (Perkins et al., 1986; Herman, 1987; Collet et al., 1998).

All six cilium structure mutants exhibited defects in sensory axon morphology that were similar to those of *tax-2* and *tax-4* mutants (phenotypes displayed in Fig. 1 and quantitated in Fig. 3A). Axon defects were observed most frequently in the ASE and ASJ neurons, and at a lower frequency in the ASI and AWB neurons (Fig. 3A; data not shown). Most or all of the defective axons observed with markers that labeled multiple cell types were accounted for by the ASE, ASJ, ASI and AWB defects, suggesting that axon defects in other amphid neurons are rare. Like *tax-2* and *tax-4* mutants, the cilium structure mutants appeared to initiate inappropriate axons: ASE, ASJ, ASI and AWB formed ectopic processes, but maintained superficially normal axons in the nerve ring. The ectopic processes were axon-like based on their accumulation of the

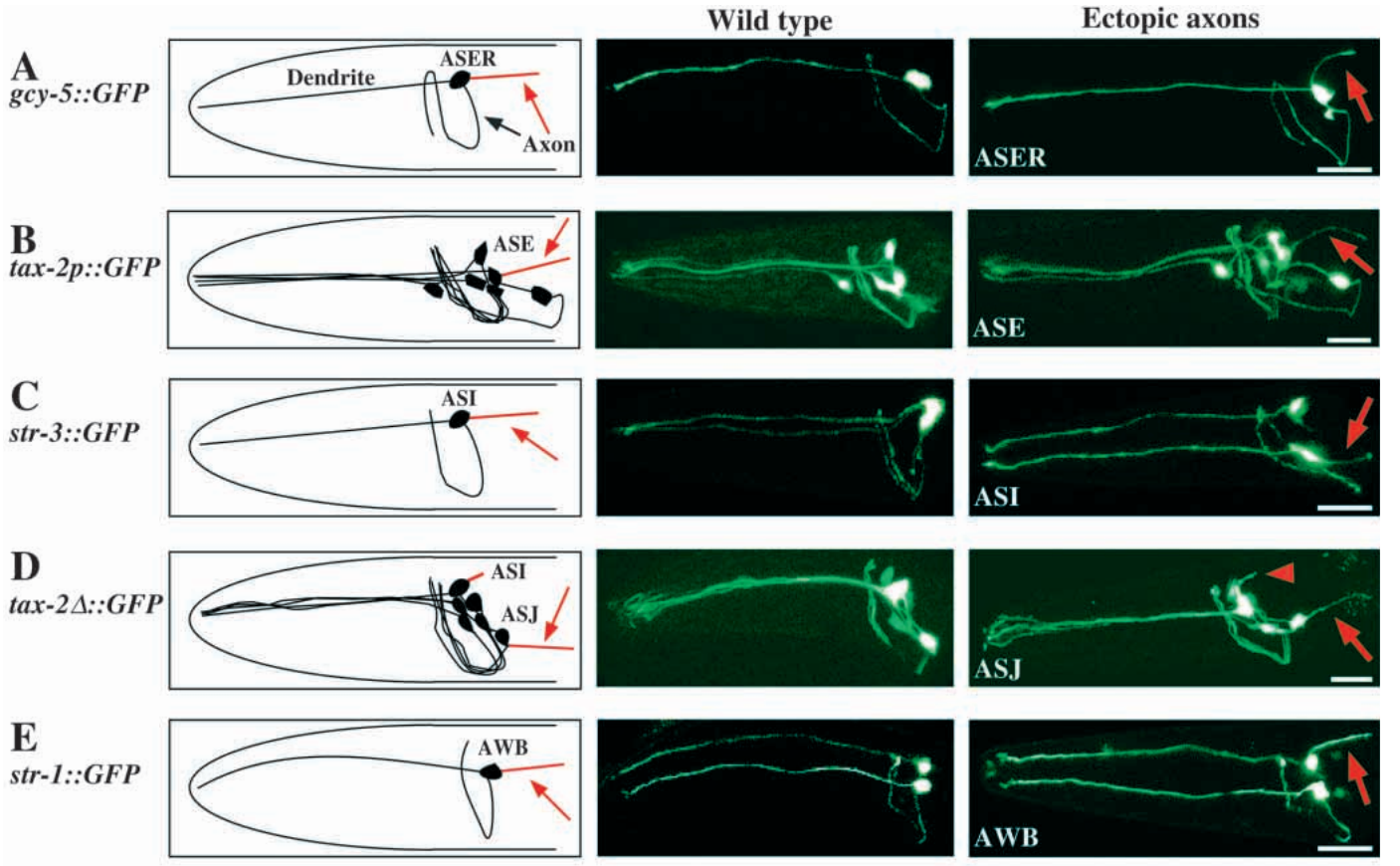

Fig. 1. Typical ectopic axons from ASE, ASI, ASJ and AWB neurons in mutants that perturb sensory neuron activity. For the ASE, ASI and AWB neurons, similar axon defects were observed for all classes of mutants described in the text (*tax-2*, *tax-4*, cilium structure mutants and channel mutants). For ASJ, all mutants were similar except *tax-2* and *tax-4* mutants, which had distinct ventral axon defects (Coburn et al., 1998). Ectopic axons projected laterally or dorsolaterally from cell bodies and could extend well posterior of the lateral ganglion into the body of the animal. Their relationship to the lateral and dorsolateral process bundles in the body has not been determined. Anterior is to the left and dorsal is up. Bars, 10 μm for all confocal images. In all cases, only one of the two bilaterally symmetric neurons in a pair is shown in the diagrams. (A) Left: diagram of ASER neuron visualized with *gcy-5:GFP*. The wild-type ASER neuron (in black) extends a dendrite to the tip of the nose and a single U-shaped axon (black arrow). Mutant ASE neurons have an ectopic axon (in red). Middle: *gcy-5::GFP* labeling of wild-type ASER neurons. Right: *gcy-5::GFP* labeling of a representative mutant animal (*che-3*). A wild-type dendrite and axon are visible, as well as a typical ectopic axon (red arrow). (B) Left: diagram of amphid neurons visualized with *tax-2p::GFP*. Mutant ASE neurons have ectopic axons (in red). Middle: *tax-2p::GFP* labeling of wild-type amphid neurons. Right: *tax-2p::GFP* labeling of a representative mutant animal (*osm-6*). A typical lateral posterior ectopic axon is visible (red arrow). (C) Left: diagram of ASI neuron visualized with *str-3::GFP*. Mutant ASI neurons have an ectopic axon (in red). Middle: *str-3::GFP* labeling of wild-type ASI neurons. Both the left and right ASI neurons are visible. Right: *str-3::GFP* labeling of a representative mutant animal (*osm-6*). A typical ectopic axon is visible (red arrow). (D) Left: Diagram of amphid neurons visualized with *tax-2Δ::GFP*. Mutant ASJ neurons have an ectopic axon (in red). Middle: *tax-2Δ::GFP* labeling of wild-type amphid neurons. Right: *tax-2Δ::GFP* labeling of a representative mutant animal (*che-3*). A typical lateral posterior ectopic axon is visible (red arrow). In addition, the ASI neuron extends a small posterior branch (red arrowhead). (E) Left: diagram of AWB neuron visualized with *str-1::GFP*. Mutant AWB neurons have an ectopic axon (in red). Middle: *str-1::GFP* labeling of wild-type AWB neurons. Both left and right AWB neurons are visible. Right: *str-1::GFP* labeling AWB in a representative mutant animal (*osm-6*). Both AWB neurons are visible. The right AWB has a typical ectopic axon (red arrow).

synaptic marker VAMP-GFP, which localizes to axons and not dendrites (Jorgensen et al., 1995), and based on their failure to accumulate dendritic markers such as olfactory receptor proteins (Dwyer et al., 1998; E. L. P., J. G. Crump, N. D. Dwyer and C. I. B., unpublished results).

Although these cilium structure mutants are defective in their chemotaxis response to a variety of volatile and water-soluble attractants (Lewis and Hodgkin, 1977; Perkins et al., 1986; Bargmann et al., 1993), they maintain a limited ability to detect high concentrations of volatile odorants such as benzaldehyde. The severity of the benzaldehyde chemotaxis defect generally correlated with the severity of the ectopic axon phenotype in different cilium structure mutants (Fig. 3B). For example, *daf-6* and *osm-1* mutants were less defective in volatile chemotaxis and axon growth than the other cilium structure mutants; *osm-5* and *osm-6* mutants were highly defective in both. This observation suggests that the sensory defect in cilia and the axon defect have a shared origin, and is consistent with a model in which the axon defects are a consequence of sensory deprivation.

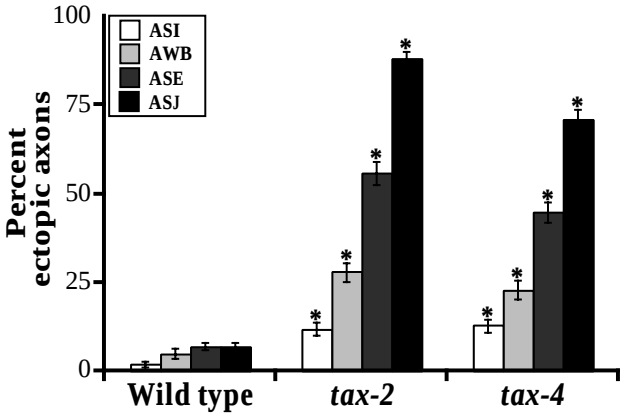

Fig. 2. *tax-2* and *tax-4* animals have defects in several amphid sensory neurons.Abnormal sensory axons resembling those in Fig. 1 were observed extending from the ASI (white bars), AWB (light gray bars) and ASE (dark gray bars) neurons (n=300 for each bar). The ventral posterior ASJ ectopic axons (black bars) have been described previously (Coburn and Bargmann, 1996; Coburn et al., 1998). *Values differ from wild type at P<0.001; error bars represent the standard error of proportion.

Mutations that affect calcium channels and membrane potential lead to ectopic sensory axons

The common phenotypes of cilium structure mutants and cyclic nucleotide-gated channel mutants suggest that altered sensory transduction disrupts sensory axon growth. In mammalian sensory systems, blocking sodium-based action potentials with tetrodotoxin leads to defects similar to those caused by sensory deprivation, implicating electrical activity in axon development (Stryker and Harris, 1986; Shatz and Stryker, 1988; Sretavan et al., 1988; Antonini and Stryker, 1993). *C. elegans* sensory neurons do not use sodium-based action potentials, but are thought to amplify excitatory potentials via opening of voltage-activated calcium channels (Goodman et al., 1998). Two different voltage-gated Ca^{2+} channel subunits, the UNC-36 α2 subunit and the EGL-19/EAT-12 α1 subunit, are widely expressed in both neurons and muscle cells and are candidates for transmitting signals between the cilia and the axons of sensory neurons (Lee et al., 1997). The *unc-36(e251)* mutation is predicted to decrease calcium channel stability and activity, and *unc-36(e251)* mutants exhibited ectopic ASE, ASI and ASJ axons that resembled those observed in cilium structure mutants (Fig. 4).

The gain-of-function mutation *egl-19(ad695)* (previously known as *eat-12*) causes delayed repolarization of pharyngeal muscle cells (Avery, 1993; Lee et al., 1997). An *egl-19::GFP* translational fusion gene is also expressed in neurons, where the same lesion might be expected to delay neuronal repolarization (Lee et al., 1997). *egl-19(ad695)* mutants had sensory axon defects that were similar to those of *unc-36* and cilium structure mutants (Fig. 4).

Although the Ca^{2+} channel mutants and the cyclic nucleotide-gated channel mutants had similar phenotypes, the defects were observed much less often in Ca^{2+} channel mutants. To ask whether these genes affect the same developmental processes, we examined amphid sensory neuron morphology in *tax-2(p691); unc-36(e251)* and *tax-2(p691); egl-19(ad695)* double mutants. The frequency of ectopic axons

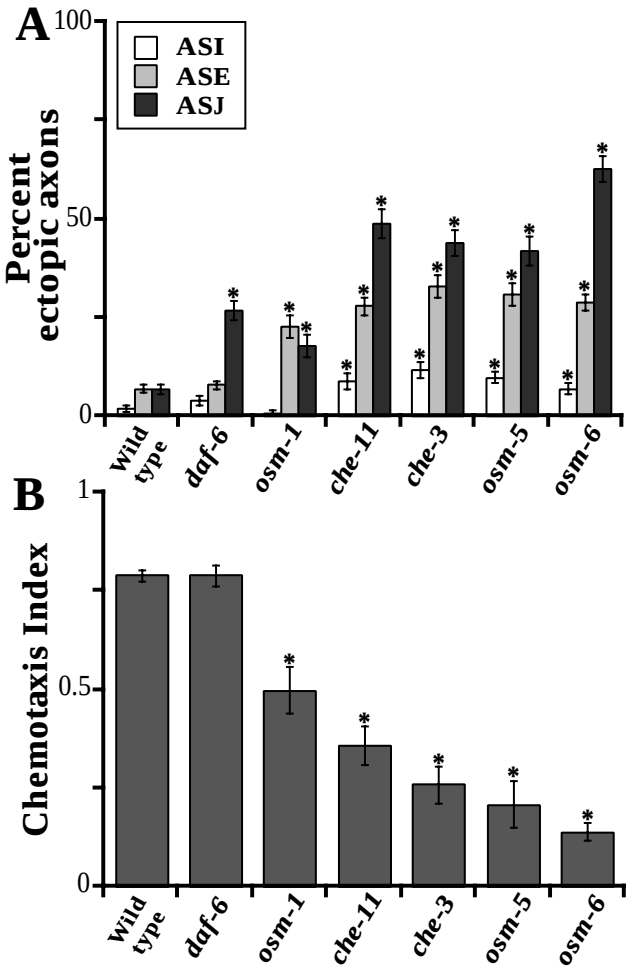

Fig. 3. Mutants with defective sensory cilia have ectopic sensory axons. (A) Six different mutants with defective sensory cilia (*daf-6, osm-1, che-11, che-3, osm-5* and *osm-6*) were examined, and the percentages of adult animals with ectopic axons in ASI (white bars), ASE (gray bars) or ASJ (black bars) neurons were determined (n=300 for each bar). Significant defects in AWB neurons were also observed in *osm-6* (9% (n=300), data not shown) and *che-3* (8% (n=300), data not shown) mutants. Error bars represent the standard error of proportion; *, values that differ from wild type at P< 0.01. (B) The extent of the chemotaxis defect in cilium structure mutants correlates with the severity of the axon defect. *daf-6, osm-1, che-11, che-3, osm-5* and *osm-6* animals were assayed for chemotaxis to benzaldehyde, a volatile chemoattractant detected by the AWC neurons. Chemotaxis indices represent the average of 5 independent assays per strain (n≥100 per assay). Values are means ± s.e.m.; *values differ from wild type at P<0.001. The cilium structure mutants were also tested for chemotaxis to the ASE chemoattractant NaCl. All cilium structure mutants were highly defective in NaCl chemotaxis, so this assay was not useful for ranking mutant severity (data not shown).

in the double mutants was the same as observed in *tax-2(p691)* mutants alone, suggesting that these genes impinge on a similar developmental process (for the ASJ neurons: *tax-2*, 88% (n=317); *unc-36*, 26% (n=336); *tax-2; unc-36*, 83% (n=325); *egl-19*, 18% (n=327); *tax-2; egl-19*, 85% (n=303)).

A mutation that affects ion gradients rather than channel activity also affects the sensory axons. EAT-6, a Na^+/K^+ATPase

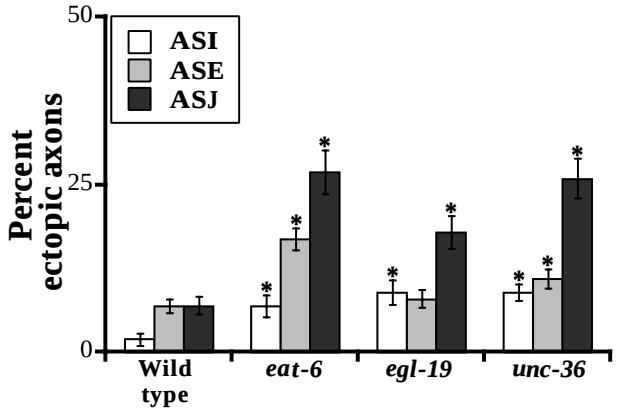

Fig. 4. Mutations that affect calcium channel activity and membrane potential lead to ectopic sensory axons. The percentage of *eat-6*, *egl-19* and *unc-36* mutants with ectopic axons in ASI (white bars), ASE (gray bars), or ASJ (black bars) neurons was determined (n=300 adults for each bar). Significant defects in AWB neurons were also observed in *eat-6* mutants (11% (n=300), data not shown). Error bars represent the standard error of proportion; *values differ from wild type at P<0.01.

pump, functions to move ions against their concentration gradients, maintaining high extracellular Na^+ and high intracellular K^+ (Avery, 1993; Davis et al., 1995). *eat-6* mutants have higher resting membrane potentials and decreased ability to form excitatory potentials in pharyngeal muscle cells. In *eat-6* mutants, ectopic sensory axons extended from the ASE, ASI and ASJ neurons (Fig. 4), all of which express *eat-6::GFP* (M. W. Davis, L. Avery, E. L. P. and C. I. B., data not shown).

To ask whether normal electrical activity of a single sensory neuron can prevent aberrant axon growth in that neuron, we expressed the *eat-6* cDNA specifically in the ASER neuron in *eat-6* mutant animals. Expression of the *eat-6* cDNA under the ASER *gcy-5* promoter restored the ASER axons to their normal morphology (*eat-6*, 20% ectopic axons (n=314); wild type, 7% (n=433); values differ at P<0.001; *eat-6; gcy-5::eat-6*, 9% (n=245); value differs from *eat-6* at P<0.001). When viewed by staining with the fluorescent dye DiO, the ASI, ASJ and AWB neurons in *eat-6; gcy-5::eat-6* animals exhibited the extra axons typically observed in *eat-6* mutants, consistent with the interpretation that activity was restored only in the ASER neuron (data not shown).

Overexpression of potassium channels can cause cell-autonomous effects on sensory axon morphology

Each of the Ca^{2+} channel genes and the *eat-6* gene described above are expressed in many cell types, raising a question about which effects are intrinsic to the affected sensory neuron. Most cilium structure genes and the cyclic nucleotide-gated channel genes are only expressed in sensory neurons, but these neurons make synaptic connections and could influence one another. Therefore, we designed an approach to silence the electrical activity of a few sensory neurons by expressing well-characterized mammalian potassium channels under cell-specific promoters.

To alter the activity of defined neurons, we expressed the rat delayed rectifying voltage-gated potassium channels Kv1.1 or Kv1.2 in the sensory neurons ASI and ASH and the PVQ interneurons using the *sra-6* promoter (Baumann et al., 1988; Tempel et al., 1988; Stuhmer et al., 1989; Troemel et al., 1995). Both Kv1.1 and Kv1.2 form channels that open upon depolarization, leading to K^+ efflux and repolarization, thus shortening and shunting excitatory potentials. The *C. elegans* genome contains several members of this highly conserved channel family, but we introduced mammalian genes because they have been extensively characterized and therefore their behavior is more predictable (Grissmer et al., 1994; Wei et al., 1996).

The *sra-6::Kv1.1* and *sra-6::Kv1.2* fusion genes were integrated into the genome, yielding two Kv1.1-expressing lines and three Kv1.2-expressing lines. Ectopic ASI axons were observed in approximately 25% of the animals in all of the integrated lines (Fig. 5A and data not shown). This effect on ASI was as severe as the effects observed in the cyclic nucleotide-gated channel mutants and in the strongest cilium structure mutants. The ASE, ASJ and AWB neurons exhibited no ectopic axons in the *sra-6::Kv1.1/1.2* lines, consistent with the predicted specificity of the *sra-6* promoter. These results suggest that a sensory neuron's morphology can be altered cell-autonomously by its own activity, though they do not exclude the possibility that non-autonomous interactions could also occur.

The *sra-6* promoter also drives expression in the ASH sensory neurons and the PVQ interneurons; the ASI neurons form no synapses with ASH or PVQ neurons (White et al., 1986). Both ASH and PVQ maintained apparently normal morphologies in the Kv1.1- and Kv1.2-expressing animals (data not shown). The normal ASH morphology is consistent with our previous observation that the cilium structure mutations and calcium channel mutations did not seem to affect this cell type. To ask whether axons in other types of neurons are sensitive to changes in electrical activity, we expressed Kv1.1 and Kv1.2 in 12 classes of interneurons and motor neurons using the *glr-1* promoter and examined these neurons using a *glr-1::gfp* fusion gene (Maricq et al., 1995). Ectopic axons were not observed in animals expressing either *glr-1::Kv1.1* or *glr-1::Kv1.2* (n=200 for each fusion gene).

To ensure that Kv1.2 potassium channel expression was influencing neuronal development by effects on neuronal activity, we constructed a predicted non-conducting version of the Kv1.2 channel by replacing the conserved GYG of the channel pore (H5) with AAA, yielding *sra-6::Kv1.2AAA* (Tinker et al., 1996). Ectopic ASI axons were not observed in animals expressing the *sra-6::Kv1.2AAA* fusion gene (Fig. 5A). Thus, the *sra-6::Kv1.1* and *sra-6::Kv1.2* fusion genes probably induce ectopic axons by allowing potassium out of the cell.

To test the functional consequences of Kv1.1 and Kv1.2 expression in sensory neurons, we examined sensory responses that are specific to the ASI and ASH neurons. Defects in the ASI neurons promote dauer larva formation, particularly in a sensitized genetic background containing an *unc-31* mutation (Avery et al., 1993). The *sra-6::Kv1.1* lines showed a partial ASI defect by this assay, with 7% (n=200) dauer larvae in an *unc-31* background (0% dauer in *sra-6::Kv1.1* alone (n=200; P<0.001), 1% in *unc-31* alone (n=200; P<0.005)). While this defect is statistically significant, a full defect in ASI function should yield 100% dauer larvae in the double mutant (Avery

et al., 1993). Similarly, *sra-6::Kv1.1* lines exhibited a partial ASH defect in osmotic avoidance and nose touch assays (10% Osm(–) (n=70), 1% Osm(–) in wild type (n=70), values differ at P<0.05; 24% Not(–) (n=280), 7% Not(–) in wild type (n=250), values differ at P<0.001). Thus, the ASH and ASI neurons were inhibited but maintained some sensory function in these strains.

Expression of the Kv1.1 and Kv1.2 channels was confirmed by antibody staining for these channels. As predicted from *sra-6::GFP* reporter gene fusions, Kv1.1 and Kv1.2 were expressed in two pairs of sensory neurons (ASH and ASI) as well as the PVQ interneurons (data not shown). Protein expression was enriched in the cell bodies.

The cilium structure and calcium channel genes act late in development to prevent ectopic axon formation

The amphid sensory neurons are born in the anterior region of the developing embryo and migrate posteriorly to their final positions, depositing dendrites as the cell bodies recede (Sulston et al., 1983). When the cell bodies arrive at their final position, they extend axons into the amphid commissure and then through the nerve ring, a process that is complete by late embryogenesis when observed by GFP labeling. In wild-type animals, sensory axon morphology appears fixed through the four larval stages and the adult stage (data not shown). The ectopic ASJ axon branches observed in *tax-2* and *tax-4* cyclic nucleotide-gated channel mutants extend during the larval stages, long after the wild-type axon has grown into the nerve ring (Coburn et al., 1998). To determine when the ectopic sensory axons in cilium structure and channel mutants develop, sensory neuron morphology was observed throughout development.

In all of the sensory mutants and channel mutants, ectopic axons first appeared in larval stages (Figs 5B, 6). The ASJ neurons were examined in *osm-6* and *che-11* animals from late embryogenesis through adulthood. In these cilium structure mutants, no extra ASJ axons were observed until the second larval stage (L2) (Fig. 6A; data not shown). The ectopic ASE and ASI axons in *osm-6* and *tax-4* also formed in mid-larval stages (Fig. 6A; data not shown). In the ion channel mutant *unc-36*, ectopic axons first appeared at the L2 stage (Fig. 6B). Similarly, ectopic ASI axons in Kv1.1- and Kv1.2-expressing animals were first observed at the L2 stage (Fig. 5B) even though the *sra-6* promoter is expressed beginning in the embryo. These results indicate that maintenance of axon morphology is disrupted by mutations in *tax-2/tax-4* genes, cilium structure genes, and ion channel genes, and by Kv1.1/1.2 expression.

Some of the axon phenotypes of the *tax-2* and *tax-4* mutants, cilium structure mutants, the ion channel mutants and the Kv1.1- and Kv1.2-expressing animals were temperature-sensitive. Ectopic axon formation was significantly greater at 25°C than at 15°C even in mutants that are null by molecular criteria (Table 2). These results suggest that an underlying axon initiation, growth or maintenance mechanism is temperature-sensitive, and that impairing sensory signal transduction reveals a temperature-sensitive process.

Some classical fast neurotransmission mutants have normal sensory development

During normal behavior, neuronal activity allows for communication with target cells primarily via neurotransmitter release. To determine whether sensory neuron development requires fast classical neurotransmission, sensory neurons were examined in synaptic transmission mutants. No sensory axon defects were observed in mutants with lesions in SNT-1, a homolog of the synaptic vesicle protein synaptotagmin, UNC-104, a kinesin that transports synaptic vesicles to the axon, or UNC-18, a conserved molecule thought to be involved in vesicle docking (Hall and Hedgecock, 1991; Otsuka et al., 1991; Hosono et al., 1992; Hata et al., 1993; Nonet et al., 1993) (Fig. 7A). All of these molecules appear to be expressed in sensory neurons, and we confirmed that UNC-104 functions in

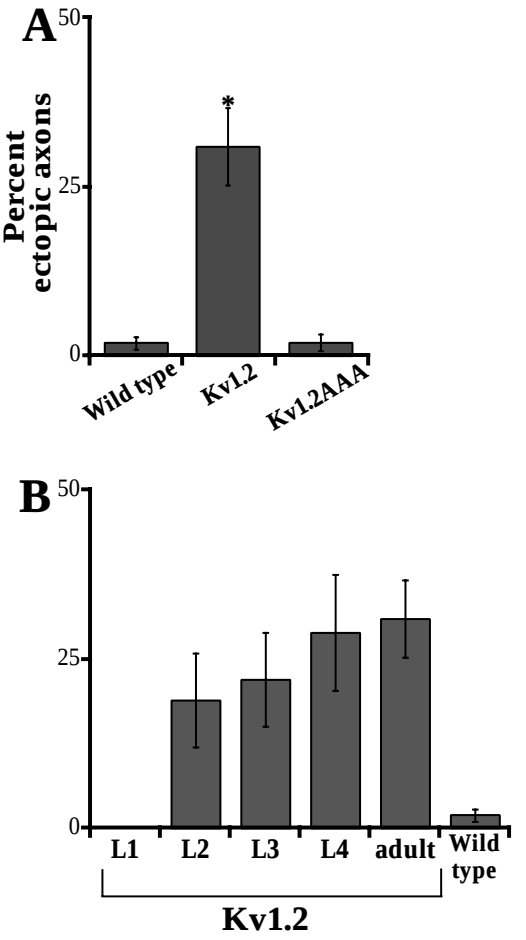

Fig. 5. Overexpression of potassium channels causes cell-autonomous axon defects in ASI sensory neurons. (A) The *sra-6* promoter was used to drive expression of the rat delayed-rectifying potassium channel Kv1.2 (Kv1.2) or a non-conducting version of this channel (Kv1.2AAA) in the ASI and ASH sensory neurons and the PVQ interneurons. Ectopic axons were observed extending only from the ASI neurons in Kv1.2-expressing animals (n=300 for each bar). The percentage of adult animals with ectopic ASI axons in one *sra-6::Kv1.2* integrated line was determined; several additional lines expressing either the *sra-6::Kv1.2* or *sra-6::Kv1.1* transgene showed similar percentages of animals with ectopic axons (data not shown). Error bars represent standard error of proportion; *values differ from wild type at P<0.001. (B) The percentage of animals with ectopic ASI axons was determined at each larval stage (L1-L4) and at the adult stage. All other amphid neurons and the PVQ interneurons appeared superficially normal. Error bars represent standard error of proportion (n=30 for each larval stage, n=300 for adults).

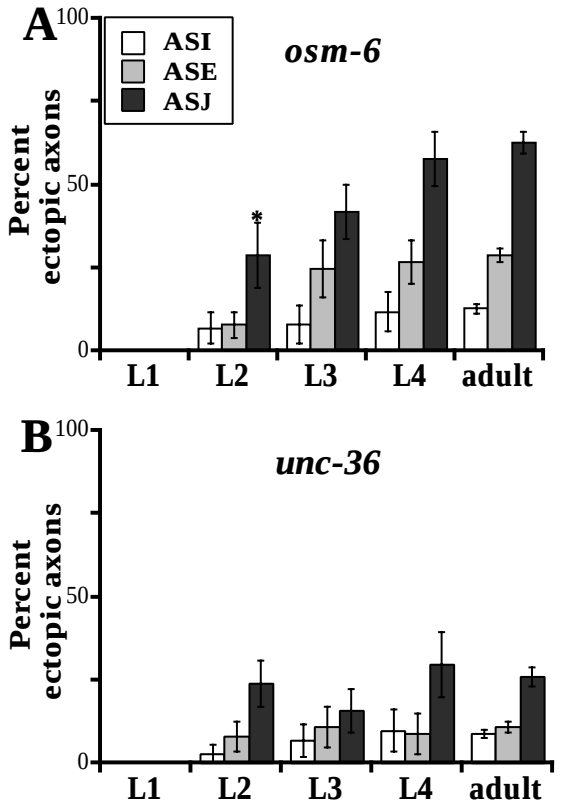

Fig. 6. Ectopic axons form late in development. (A,B) Amphid axon morphologies were examined in *osm-6* and *unc-36* mutants throughout development to determine when ectopic axons form. The percentage of animals with ectopic axons in ASI (white bars), ASE (gray bars), or ASJ (black bars) was determined at each larval stage (L1-L4) and at the adult stage. Wild-type animals were examined at each larval stage and at the adult stage and rarely exhibited ectopic axons at any stage of development (Table 2 and data not shown). Error bars represent the standard error of proportion (n=30 for each larval stage, n=300 for adults; for *osm-6* ASJ axons, L2 values differ from adult at P<0.01).

Table 2. Ectopic axon phenotypes are temperature-sensitive

	ASI		ASE		ASJ	
	25°	15°	25°	15°	25°	15°
Wild type	4±1	2±1	7±1	4±1	7±1	5±1
daf-6	4±1	3±1	8±1	6±1	27±3	10±3*
osm-1	1±1	2±1	23±3	15±3*	18±3	6±3*
che-11	9±2	2±1*	28±2	8±1*	49±4	11±2*
che-3	12±2	7±2	33±3	13±2*	44±3	10±2*
osm-5	10±2	4±1*	31±3	18±3*	42±4	9±3*
osm-6	7±1	2±1*	29±2	13±2*	63±3	14±2*
eat-6	7±1	8±2	17±2	8±2*	27±3	19±4*
egl-19	9±2	7±2	8±1	4±1	18±3	6±2*
unc-36	7±2	4±1	11±2	5±1	26±3	1±1*
tax-2	12±2	4±1*	56±3	36±3*	88±2	75±5
tax-4	13±3	3±1*	43±3	42±3	71±3	67±3
unc-13	34±5	25±3	38±3	24±3*	31±3	19±3*
sra-6::Kv1.1	25±5	6±2*	n.d.	n.d.	6±1	5±1
sra-6::Kv1.2	24±5	5±2*	n.d.	n.d.	7±1	5±1

Axon phenotypes were scored in adult animals raised at either 25°C or 15°C using GFP fusion genes *str-3::GFP* (ASI), *tax-2p::GFP* (ASE), or *tax-2Δ::GFP* (ASJ). The percentages of animals with at least one ectopic axon are tabulated.

Error values are standard error of proportion; significance was calculated by comparison of two proportions (asterisks represent values that differ between 25°C and 15°C at P<0.01).

n=300 for each value; n.d., not determined.

sensory neurons by demonstrating that synaptic vesicles were trapped in sensory cell bodies in *unc-104* mutants (J. G. Crump and C. I. B., unpublished results).

Unlike the other synaptic transmission mutants, *unc-13* mutants displayed ectopic posteriorly directed axons (Fig. 7A) that formed late in development (Fig. 7B) like those of *tax-2/tax-4* mutants, cilium structure mutants and ion channel mutants. *unc-13* encodes a conserved calcium- and phospholipid-binding protein that is implicated in exocytosis and synaptic transmission (Maruyama and Brenner, 1991; Betz et al., 1996). *unc-13* might be more defective in exocytosis than the mutants described above, or it might have defects in sensory function as well as defects in exocytosis.

DISCUSSION

Sensory deprivation causes characteristic axon defects in *C. elegans*

Although *C. elegans* traditionally is considered to be an animal with a hard-wired nervous system, our results reveal an effect of sensory activity on the morphology of *C. elegans* sensory neurons. Ectopic axon-like processes were observed in six different cilium structure mutants, providing strong evidence that sensory deprivation is sufficient to cause axon defects. Alternatively, all six genes might affect both cilium structure and axon extension directly, but this is very unlikely. In particular, the *daf-6* gene is known from genetic mosaic analysis to be active in the amphid sheath cell and not in the sensory neurons themselves (Albert and Riddle, 1983; Herman, 1987). The amphid sheath is closely associated with the cilia and the sensory pore, but not with the sensory axons, and the *daf-6* mutation probably blocks physical access of otherwise normal sensory cilia to environmental stimuli (Perkins et al., 1986; Herman, 1987). Moreover, the OSM-6 protein is localized only to cilia and not to axons, and is related to a cilium-specific gene in *Chlamydomonas* (Cole et al., 1998; Collet et al., 1998). Finally, the cilia defects in all of these mutants are distinct, ranging from complete cilia truncations to slight malformations of the cilia endings (Perkins et al., 1986), yet they all display similar axon phenotypes. While the genes other than *daf-6* and *osm-6* are less well-characterized, they all share similar axon phenotypes and cell-type specificity, arguing that all cilium structure genes impinge on a common process that indirectly affects neuron morphology.

While the case for sensory deprivation in the cilium structure mutants is strong, the electrical activity of the sensory neurons has not been observed directly in the channel mutants. Nonetheless, several arguments provide evidence that the mutants studied here do alter electrical activity. First, many of the molecules studied here have highly conserved, well-characterized mammalian counterparts. For TAX-2 and TAX-4, this predicted homology is supported by characterization of channel properties when expressed in heterologous cells

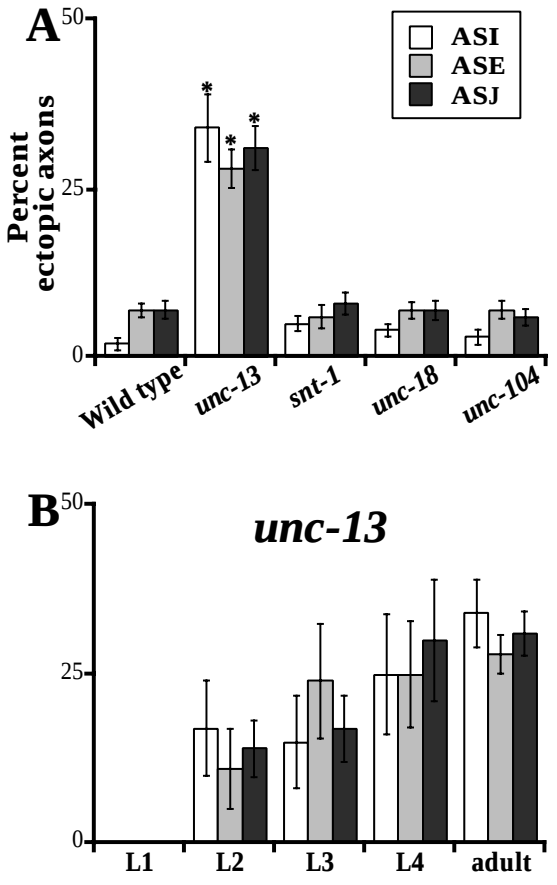

Fig. 7. Sensory neuron development is affected by *unc-13*, but not by other genes that affect classical fast neurotransmission.
(A) Percentage of ectopic axons in adult wild-type, *unc-13*, *snt-1*, *unc-18* and *unc-104* animals. Wild-type, *snt-1*, *unc-18* and *unc-104* amphid axon morphologies were indistinguishable. Ectopic axons in the ASI, ASE and ASJ neurons of *unc-13* mutants resembled those displayed in Fig. 1. Similar percentages of animals with ectopic axons in ASI (white bars), ASE (gray bars) or ASJ (black bars) neurons were observed in *unc-13(e51)* (shown here) and *unc-13(e450)* (data not shown). Error bars represent the standard error of proportion (n=300 for each strain); *values differ from wild type at P< 0.001. (B) Amphid axon morphologies were examined in *unc-13(e51)* mutants throughout development to determine when ectopic axons form. The percentage of animals with ectopic axons in ASI (white bars), ASE (gray bars) or ASJ (black bars) was determined at larval stages (L1-L4) and at the adult stage. Wild-type animals were examined at each larval stage and at the adult stage and rarely exhibited ectopic axons at any stage of development (Table 2 and data not shown). Error bars represent the standard error of proportion (n=30 for each larval stage, n=300 for adults).

(Komatsu et al., 1996, 1999). Second, several of the mutants studied here have been studied electrophysiologically in *C. elegans*, albeit in another excitable cell type. The *unc-36* and *egl-19* mutations affect pharyngeal muscle calcium channels (Lee et al., 1997) and the *eat-6* mutation in a Na^+/K^+ ATPase affects pharyngeal membrane potential and excitability (Davis et al., 1995). Third, electrophysiological analysis of the ASE sensory neurons demonstrates that voltage-dependent calcium channels and voltage-dependent potassium channels are endogenous modulators of their electrical activity (Goodman et al., 1998), indicating that the molecules studied here or related molecules are present within these neurons during normal development. Fourth, the Kv1.1 and Kv1.2 channels share strong sequence similarities with *C. elegans* potassium channels and behave properly when expressed in heterologous non-neuronal cells, suggesting that they would retain their voltage-regulated properties when expressed in *C. elegans* sensory neurons (Tempel et al., 1988; Stuhmer et al., 1989). The precise activity pattern in each mutant is not known, yet similar axon defects are caused by these varied manipulations. These observations suggest a common mechanism that is most easily explained by effects on activity.

The expression of a voltage-gated potassium channel in the ASI sensory neurons caused ectopic axon growth in a cell-autonomous fashion. Likewise, ectopic ASER axon growth is prevented by restoring the *eat-6* cDNA in the single ASER neuron in *eat-6* mutant animals. These results strongly suggest that sensory neurons are responsive to their own activity as they grow. In pharyngeal muscles, the *egl-19* mutation increases calcium channel activity (Lee et al., 1997), while the *unc-36* mutation should decrease calcium channel activity, yet in sensory neurons both mutation lead to similar axon defects. The effects of these mutations on activity might be different in the sensory neurons, which probably express fewer calcium channels than the muscles (Goodman et al., 1998), or it may be that the widely expressed calcium channel genes influence sensory neurons indirectly via other neurons, yielding complex effects.

Mutations that affect neuronal activity perturb axon initiation or growth, not axon guidance

All of the mutations described here caused ectopic axon growth at a late time in development and not during initial axon outgrowth and guidance. We propose that the sensory neurons have two distinct phases of development: initial axon outgrowth, which is independent of activity, and maintenance of sensory neuron morphology, which depends on activity. Two similar phases are found in the vertebrate visual system. For example, axon extension from the thalamus to the visual cortex is activity-independent, but axon elaboration and synaptic patterning in the target field are altered when activity is disrupted (Goodman and Shatz, 1993). Alternatively, it may be that activity does have effects in embryonic and L1 development of *C. elegans*, but that the mutations studied here do not affect the earliest forms of neuronal activity.

There are many possible mechanisms by which activity might affect axon maintenance but not axon pathfinding. Activity may allow the developing sensory neurons to communicate with and appropriately innervate their target cells. In the absence of activity, sensory neurons may have defective connections and might then extend ectopic axons in search of other targets. Another possible function for activity could be to stabilize and shape axon morphologies during growth. The initial structures of the chemosensory neurons are established before hatching, but between hatching and adulthood the animal increases its length by fivefold and its mass about 100-fold. The extensive growth of these axons presumably requires signalling to determine the position and extent of growth, but it is likely that some of the guidance cues that are present in the embryo are downregulated during larval stages (Zallen et al., 1998). Activity-dependent mechanisms

might be part of an alternative pathway that regulates axon growth during the later part of development. Activity could also be a factor in neuronal remodeling. Several axons grow into the nerve ring in the L1 stage, and the HSN axon grows in as late as the L4 stage; activity may help integrate these late-arriving axons as well as other neurons that rewire during larval stages (White et al., 1978, 1986).

Classical neurotransmission via the excitatory neurotransmitter glutamate contributes to the refinement of connections within the mammalian visual and somatosensory nervous systems (Kleinschmidt et al., 1987; Miller et al., 1989; Fox, 1992; Li et al., 1994; Fox et al., 1996). Several mutations that affect classical synaptic transmission in *C. elegans* did not affect sensory axon morphology, revealing a possible distinction between the behavior of *C. elegans* and mammalian sensory systems. *C. elegans* neurons may use some alternative form of cell communication that is modulated by activity to shape their processes, or perhaps the effects are entirely intrinsic to single sensory neurons.

Are activity-dependent processes used to control axon outgrowth of other invertebrates? Activity perturbations in *Drosophila* mechanosensory neurons and cricket cercal sensory neurons do not affect their axon morphology (Burg and Wu, 1986; Chiba and Murphey, 1991). However, striking activity-dependent effects on synapse maintenance and growth have been observed at the *Drosophila* neuromuscular junction (NMJ) (Broadie and Bate, 1993; Jarecki and Keshishian, 1995). At the NMJ, activity regulates the number of neuronal inputs per muscle fiber and the number of synapses each neuron makes. Mutations that affect the *Shaker* potassium channel, the *para* voltage-activated sodium channel, or cAMP signaling pathways regulate synaptic sprouting and other synaptic functions at the NMJ, but only during larval stages and not during its initial formation (Zhong et al., 1992; Davis and Goodman, 1998).

Sensory activity also functions in the maintenance of normal axon arbors in vertebrate sensory systems. In the cat, the organization of inputs that produce orientation columns is apparent in the visual cortex before the eyes first open. However, if the cat's eyes remain closed, orientation maps degenerate, suggesting that an absence of patterned visual activity at certain periods of development can actively disrupt rudimentary columns that did not depend on visual input for their formation (Crair et al., 1998).

Our results indicate that the regulation of neuronal morphology by activity is present in both vertebrate and invertebrate sensory systems. We suggest that *C. elegans* relies on neural activity in a maintenance or feedback mechanism during larval growth. It may be that activity-dependent pathways first evolved as part of a general homeostatic mechanism that was later recruited to refine projections of large axon groups in complex nervous systems. The neurons described here provide an opportunity to examine mechanisms that couple neuronal activity to neuronal morphology in a simple, genetically accessible system.

We thank Shannon Grantner and Yongmei Zhang for excellent technical support and Timothy Yu for help with confocal microscopy. We are grateful to David McKinnon for generously providing Kv1.1 and Kv1.2 constructs, Wayne Davis and Leon Avery for the *eat-6::GFP*-expressing strain, and Andrew Fire for the expression constructs. We are indebted to Michael Stryker and Lee Honigberg as well as Susan Kirch, Erik Lundquist, Timothy Yu, J. Gage Crump and other members of the Bargmann laboratory for their comments on the manuscript and for suggestions during the course of this work. Some of the strains used in this study were obtained from the Caenorhabditis Genetics Center, which is funded by the National Institutes of Health National Center for Research Resources. This work was supported by the Howard Hughes Medical Institute. E.L.P was supported by a research fellowship from the American Heart Association, California Affiliate, J.A.Z. was supported by an NSF Predoctoral Fellowship, and C.I.B. is an Assistant Investigator of the Howard Hughes Medical Institute.

REFERENCES

Albert, P. S. and Riddle, D. L. (1983). Developmental alterations in sensory neuroanatomy of the *Caenorhabditis elegans* dauer larva. *J. Comp. Neurol.* **219,** 461-481.

Antonini, A. and Stryker, M. P. (1993). Development of individual geniculocortical arbors in cat striate cortex and effects of binocular impulse blockade. *J. Neurosci.* **13,** 3549-3573.

Avery, L. (1993). The genetics of feeding in *Caenorhabditis elegans*. *Genetics* **133,** 897-917.

Avery, L., Bargmann, C. I. and Horvitz, H. R. (1993). The *Caenorhabditis elegans unc-31* gene affects multiple nervous system-controlled functions. *Genetics* **134,** 455-464.

Bargmann, C. I., Hartwieg, E. and Horvitz, H. R. (1993). Odorant-selective genes and neurons mediate olfaction in *C. elegans*. *Cell* **74,** 515-527.

Bargmann, C. I. and Mori, I. (1997). Chemotaxis and thermotaxis. In *C. elegans II*, (ed. D. L. Riddle, T. Blumenthal, B. J. Meyer and J. R. Priess), pp. 717-737. Plainview: Cold Spring Harbor Press.

Baumann, A., Grupe, A., Ackermann, A. and Pongs, O. (1988). Structure of the voltage-dependent potassium channel is highly conserved from *Drosophila* to vertebrate central nervous systems. *EMBO J.* **7,** 2457-2463.

Betz, A., Telemenakis, I., Hofmann, K. and Brose, N. (1996). Mammalian *unc-13* homologues as possible regulators of neurotransmitter release. *Biochem Soc Trans* **24,** 661-666.

Brenner, S. (1974). The genetics of *Caenorhabditis elegans*. *Genetics* **77,** 71-94.

Broadie, K. and Bate, M. (1993). Activity-dependent development of the neuromuscular synapse during *Drosophila* embryogenesis. *Neuron* **11,** 607-619.

Burg, M. G. and Wu, C. F. (1986). Differentiation and central projections of peripheral sensory cells with action-potential block in *Drosophila* mosaics. *J. Neurosci.* **6,** 2968-2976.

Chiba, A. and Murphey, R. K. (1991). Connectivity of identified central synapses in the cricket is normal following regeneration and blockade of presynaptic activity. *J. Neurobiol.* **22,** 130-142.

Coburn, C. M. and Bargmann, C. I. (1996). A putative cyclic nucleotide-gated channel is required for sensory development and function in *C. elegans*. *Neuron* **17,** 695-706.

Coburn, C. M., Mori, I., Ohshima, Y. and Bargmann, C. I. (1998). A cyclic nucleotide-gated channel inhibits sensory axon outgrowth in larval and adult *Caenorhabditis elegans*: a distinct pathway for maintenance of sensory axon structure. *Development* **125,** 249-258.

Cole, D. G., Deiner, D. R., Himelblau, A. L., Beech, P. L., Fuster, J. C. and Rosenbaum, J. L. (1998). *Chlamydomonas* kinesin-II-dependent intraflaggellar transport (IFT): IFT particles contain proteins required for cilia assembly in *Caenorhabditis elegans* sensory neurons. *J. Cell Biol.* **141,** 993-1008.

Collet, J., Spike, C. A., Lundquist, E. A., Shaw, J. E. and Herman, R. K. (1998). Analysis of *osm-6*, a gene that affects sensory cilium structure and sensory neuron function in *Caenorhabditis elegans*. *Genetics* **148,** 187-200.

Crair, M. C., Gillespie, D. C. and Stryker, M. P. (1998). The role of visual experience in the development of columns in cat visual cortex. *Science* **279,** 566-570.

Davis, G. W. and Goodman, C. S. (1998). Synapse-specific control of synaptic efficacy at the terminals of a single neuron. *Nature* **392,** 82-86.

Davis, M. W., Somerville, D., Lee, R. Y., Lockery, S., Avery, L. and Fambrough, D. M. (1995). Mutations in the *Caenorhabditis elegans* Na,K-ATPase alpha-subunit gene, *eat-6*, disrupt excitable cell function. *J. Neurosci.* **15,** 8408-8418.

Dwyer, N. D., Troemel, E. R., Sengupta, P. and Bargmann, C. I. (1998). Odorant receptor localization to olfactory cilia is mediated by ODR-4, a novel membrane-associated protein. *Cell* **93,** 455-466.

Fox, K. (1992). A critical period for experience-dependent synaptic plasticity in rat barrel cortex. *J. Neurosci.* **12,** 1826-1838.

Fox, K., Schlaggar, B. L., Glazewski, S. and O'Leary, D. D. (1996). Glutamate receptor blockade at cortical synapses disrupts development of thalamocortical and columnar organization in somatosensory cortex. *Proc. Natl. Acad. Sci. USA* **93,** 5584-5589.

Goodman, C. S. and Shatz, C. J. (1993). Developmental mechanisms that generate precise patterns of neuronal connectivity. *Cell* **72,** 77-98.

Goodman, M. B., Hall, D. H., Avery, L. and Lockery, S. R. (1998). Active currents regulate sensitivity and dynamic range in *C. elegans* neurons. *Neuron* **20,** 763-772.

Grissmer, S., Nguyen, A. N., Aiyar, J., Hanson, D. C., Mather, R. J., Gutman, G. A., Karmilowicz, M. J., Auperin, D. D. and Chandy, K. G. (1994). Pharmacological characterization of five cloned voltage-gated K^+ channels, types Kv1.1, 1.2, 1.3, 1.5, and 3.1, stably expressed in mammalian cell lines. *Mol. Pharmacol.* **45,** 1227-1234.

Hall, D. H. and Hedgecock, E. M. (1991). Kinesin-related gene *unc-104* is required for axonal transport of synaptic vesicles in *C. elegans*. *Cell* **65,** 837-847.

Harris, R. M. and Woolsey, T. A. (1981). Dendritic plasticity in mouse barrel cortex following postnatal vibrissa follicle damage. *J. Comp. Neurol.* **196,** 357-376.

Hata, Y., Slaughter, C. A. and Sudhof, T. C. (1993). Synaptic vesicle fusion complex contains *unc-18* homologue bound to syntaxin. *Nature* **366,** 347-351.

Herman, R. K. (1987). Mosaic analysis of two genes that affect nervous system structure in *Caenorhabditis elegans*. *Genetics* **116,** 377-388.

Herman, R. K. and Hedgecock, E. M. (1990). Limitation of the size of the vulval primordium of *Caenorhabditis elegan*s by *lin-15* expression in surrounding hypodermis. *Nature* **348,** 169-171.

Hosono, R., Hekimi, S., Kamiya, Y., Sassa, T., Murakami, S., Nishiwaki, K., Miwa, J., Taketo, A. and Kodaira, K. I. (1992). The *unc-18* gene encodes a novel protein affecting the kinetics of acetylcholine metabolism in the nematode *Caenorhabditis elegans*. *J. Neurochem.* **58,** 1517-1525.

Huang, L. S., Tzou, P. and Sternberg, P. W. (1994). The *lin-15* locus encodes two negative regulators of *Caenorhabditis elegans* vulval development. *Mol. Biol. Cell* **5,** 395-411.

Hubel, D. H., Wiesel, T. N. and LeVay, S. (1977). Plasticity of ocular dominance columns in monkey striate cortex. *Philos. Trans. R. Soc. Lond. B Biol. Sci.* **278,** 377-409.

Jarecki, J. and Keshishian, H. (1995). Role of neural activity during synaptogenesis in Drosophila. *J. Neurosci.* **15,** 8177-8190.

Jorgensen, E. M., Hartwieg, E., Schuske, K., Nonet, M. L., Jin, Y. and Horvitz, H. R. (1995). Defective recycling of synaptic vesicles in synaptotagmin mutants of *Caenorhabditis elegans*. *Nature* **378,** 196-199.

Kaplan, J. M. and Horvitz, H. R. (1993). A dual mechanosensory and chemosensory neuron in *Caenorhabditis elegans*. *Proc. Natl. Acad. Sci. USA* **90,** 2227-2231.

Kleinschmidt, A., Bear, M. F. and Singer, W. (1987). Blockade of 'NMDA' receptors disrupts experience-dependent plasticity of kitten striate cortex. *Science* **238,** 355-358.

Komatsu, H., Jin, Y.H., L'Etoile, N., Mori, I., Bargmann, C.I., Akaike, N. and Ohshima, Y. (1999). Functional reconstitution of a heteromeric cyclic nucleotide-gated channel of *C. elegans* in cultured cells. *Brain Res.* (in press).

Komatsu, H., Mori, I., Rhee, J. S., Akaike, N. and Ohshima, Y. (1996). Mutations in a cyclic nucleotide-gated channel lead to abnormal thermosensation and chemosensation in *C. elegans*. *Neuron* **17,** 707-718.

Lee, R. Y., Lobel, L., Hengartner, M., Horvitz, H. R. and Avery, L. (1997). Mutations in the alpha1 subunit of an L-type voltage-activated Ca^{2+} channel cause myotonia in *Caenorhabditis elegans*. *EMBO J.* **16,** 6066-76.

LeVay, S., Wiesel, T. N. and Hubel, D. H. (1980). The development of ocular dominance columns in normal and visually deprived monkeys. *J. Comp. Neurol.* **191,** 1-51.

Lewis, J. A. and Hodgkin, J. A. (1977). Specific neuroanatomical changes in chemosensory mutants of the nematode *Caenorhabditis elegans*. *J. Comp. Neurol.* **172,** 489-510.

Li, Y., Erzurumlu, R. S., Chen, C., Jhaveri, S. and Tonegawa, S. (1994). Whisker-related neuronal patterns fail to develop in the trigeminal brainstem nuclei of NMDAR1 knockout mice. *Cell* **76,** 427-437.

Maricq, A. V., Peckol, E., Driscoll, M. and Bargmann, C. I. (1995) Mechanosensory signalling in *C. elegans* mediated by the GLR-1 glutamate receptor. *Nature* **378,** 78-81.

Maruyama, I. N. and Brenner, S. (1991). A phorbol ester/diacylglycerol-binding protein encoded by the *unc-13* gene of *Caenorhabditis elegans*. *Proc. Natl. Acad. Sci. USA* **88,** 5729-5733.

Miller, D. M. and Shakes, D. C. (1995). Immunofluorescence microscopy. In *Caenorhabditis elegans: Modern Biological Analysis of an Organism*, vol. 48 (ed. H. F. Epstein and D. C. Shakes), pp. 365-394. San Diego: Academic Press, Inc.

Miller, K. D., Chapman, B. and Stryker, M. P. (1989). Visual responses in adult cat visual cortex depend on N-methyl-D-aspartate receptors. *Proc. Natl. Acad. Sci. USA* **86,** 5183-5187.

Nonet, M. L., Grundahl, K., Meyer, B. J. and Rand, J. B. (1993). Synaptic function is impaired but not eliminated in *C. elegans* mutants lacking synaptotagmin. *Cell* **73,** 1291-1305.

Otsuka, A. J., Jeyaprakash, A., Garcia-Anoveros, J., Tang, L. Z., Fisk, G., Hartshorne, T., Franco, R. and Born, T. (1991). The *C. elegans unc-104* gene encodes a putative kinesin heavy chain-like protein. *Neuron* **6,** 113-122.

Perkins, L. A., Hedgecock, E. M., Thomson, J. N. and Culotti, J. G. (1986). Mutant sensory cilia in the nematode *Caenorhabditis elegans*. *Dev. Biol.* **117,** 456-487.

Sengupta, P., Chou, J. H. and Bargmann, C. I. (1996). *odr-10* encodes a seven transmembrane domain olfactory receptor required for responses to the odorant diacetyl. *Cell* **84,** 899-909.

Shatz, C. J. (1994). Viktor Hamburger Award review. Role for spontaneous neural activity in the patterning of connections between retina and LGN during visual system development. *Int. J. Dev. Neurosci*. **12,** 531-546.

Shatz, C. J. (1996). Emergence of order in visual system development. *Proc. Natl. Acad. Sci. USA* **93,** 602-608.

Shatz, C. J. and Stryker, M. P. (1978). Ocular dominance in layer IV of the cat's visual cortex and the effects of monocular deprivation. *J. Physiol.* **281,** 267-283.

Shatz, C. J. and Stryker, M. P. (1988). Prenatal tetrodotoxin infusion blocks segregation of retinogeniculate afferents. *Science* **242,** 87-89.

Sretavan, D. W., Shatz, C. J. and Stryker, M. P. (1988). Modification of retinal ganglion cell axon morphology by prenatal infusion of tetrodotoxin. *Nature* **336,** 468-471.

Starich, T. A., Herman, R. K., Kari, C. K., Yeh, W. H., Schackwitz, W. S., Schuyler, M. W., Collet, J., Thomas, J. H. and Riddle, D. L. (1995). Mutations affecting the chemosensory neurons of *Caenorhabditis elegans*. *Genetics* **139,** 171-188.

Stryker, M. P. and Harris, W. A. (1986). Binocular impulse blockade prevents the formation of ocular dominance columns in cat visual cortex. *J. Neurosci.* **6,** 2117-2133.

Stuhmer, W., Ruppersberg, J. P., Schroter, K. H., Sakmann, B., Stocker, M., Giese, K. P., Perschke, A., Baumann, A. and Pongs, O. (1989). Molecular basis of functional diversity of voltage-gated potassium channels in mammalian brain. *EMBO J.* **8,** 3235-3244.

Sulston, J. E., Schierenberg, E., White, J. G. and Thomson, J. N. (1983). The embryonic cell lineage of the nematode *Caenorhabditis elegans*. *Dev. Biol.* **100,** 64-119.

Tempel, B. L., Jan, Y. N. and Jan, L. Y. (1988). Cloning of a probable potassium channel gene from mouse brain. *Nature* **332,** 837-839.

Tinker, A., Jan, Y. N. and Jan, L. Y. (1996). Regions responsible for the assembly of inwardly rectifying potassium channels. *Cell* **87,** 857-868.

Troemel, E. R., Chou, J. H., Dwyer, N. D., Colbert, H. A. and Bargmann, C. I. (1995). Divergent seven transmembrane receptors are candidate chemosensory receptors in *C. elegans*. *Cell* **83,** 207-218.

Troemel, E. R., Kimmel, B. E. and Bargmann, C. I. (1997). Reprogramming chemotaxis responses: sensory neurons define olfactory preferences in *C. elegans*. *Cell* **91,** 161-169.

Vowels, J. J. and Thomas, J. H. (1994). Multiple chemosensory defects in *daf-11* and *daf-21* mutants of *Caenorhabditis elegans*. *Genetics* **138,** 303-316.

Ward, S., Thomson, N., White, J. G. and Brenner, S. (1975). Electron microscopical reconstruction of the anterior sensory anatomy of the nematode *Caenorhabditis elegans*. *J. Comp. Neurol.* **160,** 313-337.

Ware, R. W., Clark, D., Crossland, K., Russell, R. L. (1975). The nerve ring of the nematode *Caenorhabditis elegans*: sensory input and motor output. *J. Comp. Neurol.* **162,** 71-110.

Wei, A., Jegla, T. and Salkoff, L. (1996). Eight potassium channel families revealed by the *C. elegans* genome project. *Neuropharmacology* **35,** 805-829.

White, J. G., Albertson, D. G. and Aness, M. A. R. (1978). Connectivity changes in a class of motoneurone during the development of a nematode. *Nature* **271,** 764-766.

White, J. G., Southgate, E., Thomson, J. N. and Brenner, S. (1986). The structure of the nervous system of the nematode *Caenorhabditis elegans*. *Philos. Trans. R. Soc. Lond. B Biol. Sci.* **314,** 1-340.

Yu, S., Avery, L., Baude, E. and Garbers, D. L. (1997). Guanylyl cyclase expression in specific sensory neurons: a new family of chemosensory receptors. *Proc. Natl. Acad. Sci. USA* **94,** 3384-3387.

Zallen, J. A., Yi, B. A. and Bargmann, C. I. (1998). The conserved immunoglobulin superfamily member SAX-3/Robo directs multiple aspects of axon guidance in *C. elegans*. *Cell* **92,** 217-227.

Zhong, Y., Budnik, V. and Wu, C. F. (1992). Synaptic plasticity in *Drosophila* memory and hyperexcitable mutants: role of cAMP cascade. *J. Neurosci.* **12,** 644-651.